Mon. Not. R. astr. Soc. (1983) **205**, 625–636

Long-baseline interferometry with a portable antenna at 81.5 MHz

J. S. Hartas★, W. G. Rees, P. F. Scott and P. J. Duffett-Smith *Mullard Radio Astronomy Observatory, Cavendish Laboratory, Madingley Road, Cambridge CB3 0HE*

Received 1983 February 21; in original form 1983 January 28

Summary. We have observed four bright radio sources with a single interferometer of variable spacing to investigate the feasibility of mapping sources with sub-arcsecond resolution at metre wavelengths. The interferometer consisted of the Cambridge 36 000-m^2 array together with a portable outstation which we used on 11 baselines from 0.5 to 1500 km. Our measurements of the fringe visibility function show that a large proportion of the emission from otherwise compact radio sources originates in extended structure which, in the cases of 3C 48 and 216, may be several hundred kiloparsecs in extent.

1 Introduction

There is increasing evidence that many 'compact' radio sources possess weak extended structure which is often difficult to map because of its low surface brightness (Duffett-Smith 1980; Winter *et al.* 1980; Laing 1981; Perley 1982). This structure usually exhibits a steeper spectral index than the compact component, so that it is more readily observed at low frequencies where its relative contribution to the total flux density is greater. The Jodrell Bank MERLIN interferometer has already had considerable success in observing such structure at 408 MHz (e.g. Lonsdale & Morison 1980) but more may be achieved at a lower frequency still. Although some long-baseline studies have been made at frequencies below 150 MHz (e.g. Clark *et al.* 1975), the largest body of high-resolution information at metre wavelengths comes at present from interplanetary scintillation observations (IPS; e.g. Readhead & Hewish 1974). This technique is efficient at collecting data, and can be used to deduce statistical information about faint radio sources which cannot be obtained in other ways, but it provides only limited information about the structure of an individual radio source. In an attempt to gain more detailed knowledge we have begun a programme of long-baseline observations at 81.5 MHz which will eventually yield maps with sub-arcsecond resolution.

Long-baseline interferometry has generally been carried out between fixed elements from which the signals have either been transmitted via radio links and correlated in real

★ Present address: John Bell Technical Systems Ltd, 127–147 Fleet Road, Fleet, Hants GU13 8PD.

time (e.g. MERLIN), or recorded with accurate timing for later playback and correlation (e.g. very long-baseline interferometry, VLBI). In either case the choice of antennas is limited by what is available, so the coverage of the $u-v$ plane is necessarily incomplete. Further, the calibration of each baseline is different because of the dissimilar antennas in use at each site. In a pioneering experiment, Allen *et al.* (1962) used a radio-link interferometer on four baselines to measure the fringe visibilities of 384 radio sources at 159 MHz. The major uncertainty in their results arose directly from the difficulty of finding the relative calibration factors for each baseline. We have devised a new technique which overcomes these problems by using a large fixed antenna at the home station together with a portable antenna at the remote station which we can position to optimize the coverage of the $u-v$ plane. We use the VLBI method of recording and playback, and calibration is straightforward since exactly the same equipment is used on each baseline and the system temperatures are dominated by unchanging galactic emission. In this paper we describe a preliminary investigation into the problems of making such measurements at low frequencies in which four bright 3C radio sources were observed at transit on 11 baselines ranging from 0.5 to 1500 km, using simple and inexpensive equipment. The results demonstrate that long-baseline interferometry is possible at metre wavelengths on a frequency which is not reserved for radio astronomy except near Cambridge, and that the effects of the ionosphere and interplanetary medium on the fringe amplitudes can be allowed for. There is strong evidence of extended emission in each of the sources which may be several hundred kpc in size for 3C 48 and 216.

2 Practical details

The interferometer (see Fig. 1) consisted of the Cambridge 3.6-hectare array (Duffett-Smith, Purvis & Hewish 1980) together with a small portable array of 8 or 16 Yagi antennas arranged in two separate east–west rows of 4 or 8, the rows being set to observe in orthogonal polarizations. For baselines greater than about 600 km the fringe amplitudes of most of the sources were expected to decrease rapidly and the larger array was used to improve the sensitivity. Two polarizations were observed simultaneously in order to allow for differential Faraday rotation in the ionosphere between the two ends of the interferometer when the baseline was longer than about 50 km. The Yagi antennas were erected to point at the zenith, giving each row a voltage pattern about 80° wide (FWHM) in the north–south direction and about 20° (or 10° using 16 antennas) in the east–west direction. Our observing time was limited by the beam pattern of the 3.6-hectare array to 100 s about meridian transit at Cambridge so it was unnecessary to arrange for tracking at the outstation. Only on the baseline to Mallorca did we need to point the beam away from the zenith by electrically phasing the individual antennas. The effective area of the outstation was about 50 m^2 (or 100 m^2) in each polarization giving an equivalent collecting area for the interferometer of about 1000 m^2 (or 1400 m^2).

The portable array was transported on a purpose-built trailer light enough to be towed by a van or small truck. We installed the recording terminal in a motor caravan so that all that was needed at any site was a domestic electricity supply and sufficient ground area on which to set up the array. Observations could generally be made within six hours of arrival at a site.

The receiving and recording equipment was planned with economy in mind since it was felt that capital outlay on elaborate equipment was inappropriate until the feasibility of low-frequency long-baseline interferometry of this sort had been established. We used double-sideband receivers with a total radio frequency bandwidth of 200 kHz centred on 81.5 MHz, giving a video band, after filtering, from 10 to 95 kHz. This narrow band kept the risk of

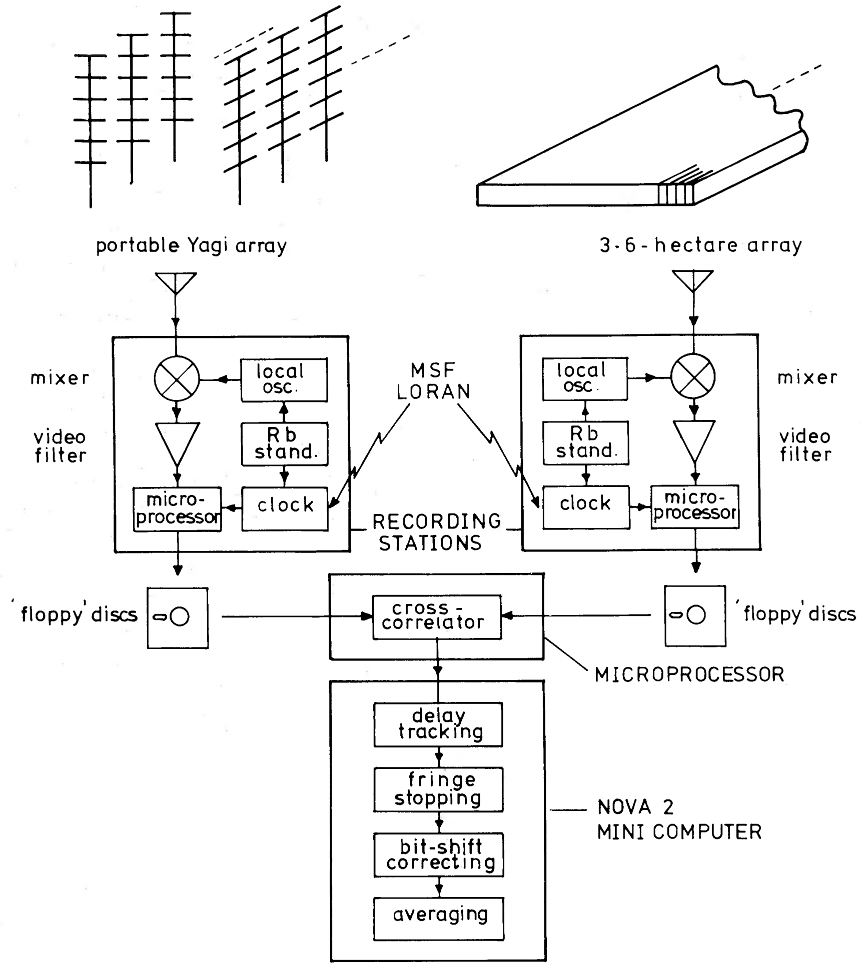

Figure 1. Block diagram of the long-baseline interferometer.

interference to a minimum and allowed us to use inexpensive audio amplifer technology in the receiver. The video output, amplified and stabilized by automatic gain control, was sampled at 200kHz and the samples converted to 1-bit digits, the usual practice in VLBI experiments; this resulted in a degradation of the signal-to-noise ratio by a factor of $2/\pi$ but minimized the quantity of data that had to be handled. The data were recorded on to floppy discs by standard microcomputers, these providing inexpensive systems with built-in error checking facilities. We were able to record continuously for the 100-s period when the source was in the interferometer beam; two separate channels were recorded simultaneously at each site, corresponding to the two polarizations at the remote station and to 'sine' and 'cosine' (signals in phase-quadrature) at the home station.

The local oscillator of each receiver was phase locked to a rubidium frequency standard whose stability (a few parts in 10^{11}) was sufficient to allow coherent integration for at least 100 s. The standards also supplied the reference signals for the clocks which were synchronized, within the United Kingdom, to the standard time transmissions at 60 kHz from MSF Rugby (National Physical Laboratory), and in France and Spain to the 100-kHz LORAN-C transmissions (United States Coast Guard). We could generally synchronize the clocks at the two ends of the interferometer to within 30 μs. Although it was always possible to synchronize the remote clock from cold, we nevertheless incorporated a battery back-up system to keep the frequency standard and clock in continuous operation during transit between sites.

The initial data reduction, consisting of playback, correlation and short time-scale integration (0.167 s), was carried out in software by the same microcomputers as were used for recording. The correlated data were transferred to a minicomputer for fringe stopping, integration (100 s), and, for the longest baselines, adjustments for delay variations. The changing ionosphere made it necessary to search in fringe frequency over a window up to 0.3 Hz wide; by fitting a linearly-varying fringe rate, we could compensate for changes in both the ionosphere and the source baseline geometry. An interpolation of delays gave the peak of the cross-correlation function, the final visibility being found from a combination of the two polarizations. We were thus able to remove completely the effects of differential Faraday rotation. Plots of the cross-correlation function versus delay and of the amplitude and phase versus time were produced to check that the reduction procedure had been successful.

The sensitivity of the system was such that we could measure the fringe visibility of 3C 48 (73.2 Jy at 81.5 MHz) with a signal-to-rms noise ratio of about 50 : 1 in the absence of scintillation on short baselines in 100 s, using eight antennas in each polarization at the remote site.

3 The observations

We observed a total of 33 of the brightest 3C radio sources between 1981 June and 1982 September. The results will be analysed in detail elsewhere; here we present our measure-

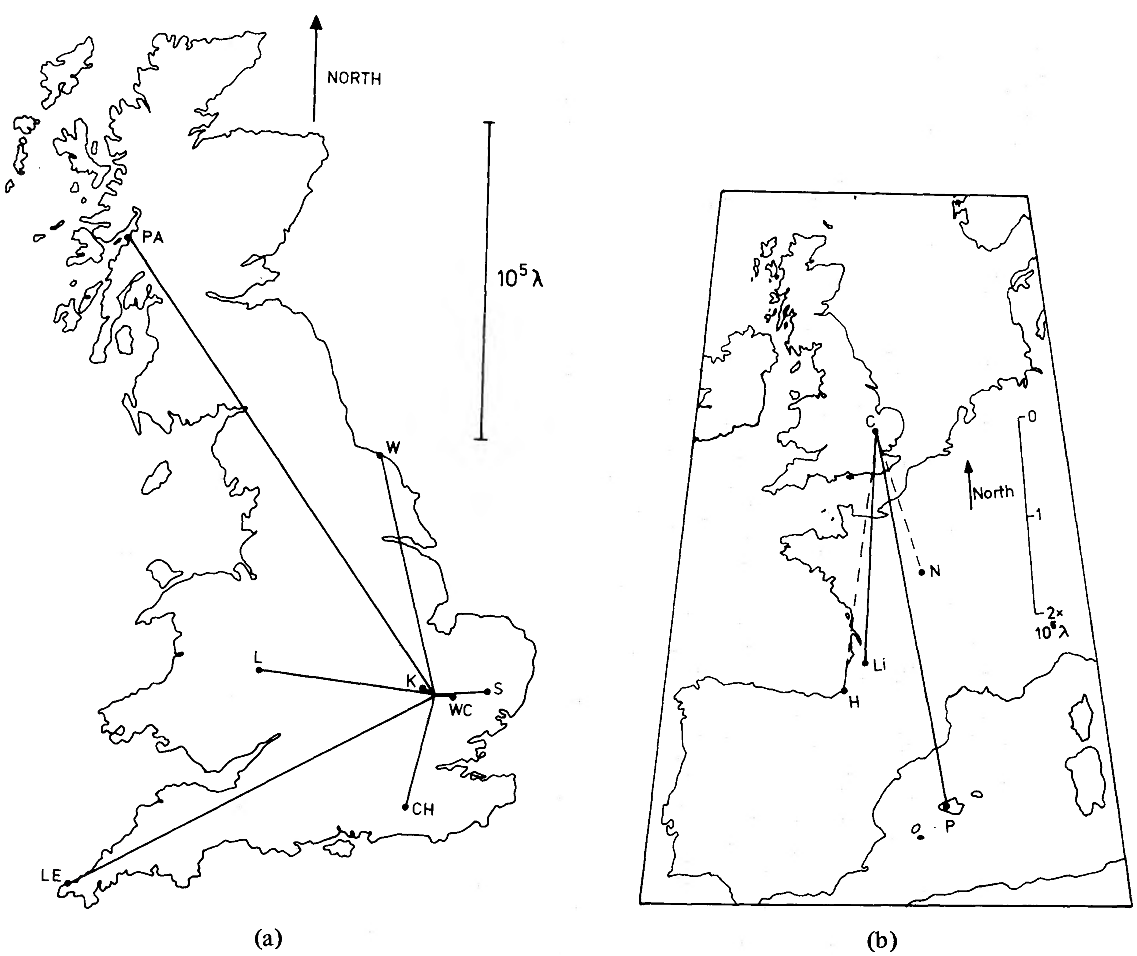

Figure 2. The baselines (a) within the UK and (b) within Europe.

ments of the fringe visibilites of four of the sources selected from the catalogue of Readhead & Hewish (1974) as exhibiting interplanetary scintillation (and therefore compact structure). We used nine baselines extending from 0.5 to 600 km for most of the sources, with two additional baselines of 900 and 1500 km for the two most compact objects 3C 48 and 147. We also attempted observations at two other sites in France (Nançay and Hendaye) but were unable to make useful recordings because of very strong local interference. We chose the baselines only for their length and their remoteness from urban areas, the exact sites (see Fig. 2) depending on the locations of friends, relatives and willing landowners. Details of the baselines are given in Table 1 where the location, date of observation, baseline length and baseline azimuth are recorded. We measured the position of each outstation to within about 10 wavelengths from domestic 1 : 50 000 survey maps.

Details of the observations of each source are given in Table 2. Here, the projected baseline length is tabulated together with the solar elongation at the time of observation (from which the effect of IPS can be deduced), the number, N, of independent observations made (spaced one day apart), the measured average fringe amplitude (in arbitrary but internally consistent units) and the rms error in each observation divided by $\sqrt{N}$. The results are also shown in Fig. 3 where the fringe visibility, normalized to the fringe amplitude measured at the shortest spacing, is plotted for each source against projected baseline length. Individual measurements of 3C 48 are plotted in Fig. 4 to demonstrate their day-to-day consistency over the whole range of baselines.

We identified several potential sources of systematic error including:

(a) faults developing in the remote station as it moved from location to location;
(b) confusion from nearby sources and solar inteference;
(c) man-made interference;
(d) decorrelation due to the ionosphere and the interplanetary medium.

We minimized the first effect by making rigorous checks of the equipment after setting up a remote station; the fact that the visibilities of unresolved sources showed no sudden variations despite the random order of baseline lengths seems to indicate the success of the checking procedure. The second source of error was a potential problem on the shortest baselines where geometrical delays were small. We checked for confusing sources in the 6C survey of radio sources (J. E. Baldwin, private communication) and for signs of interference

Table 1. Baseline details.

Remote location	Code	Date	Baseline length (λ)	Baseline azimuth (°)	Comment
Lords Bridge	LB	82 June	~ 130	90	'Zero' baseline
Kingston	K	81 June	1 350	281	
Weston Colville	WC	81 June	6 360	98	
Stowmarket	S	81 July	16 830	87	
Christ's Hospital	CH	81 Sept	34 970	194	
Ludlow	L	81 Nov	50 600	274	
Whitby	W	81 Sept	72 140	346	
Lands End	LE	82 Jan	121 070	243	
Port Appin	PA	81 Oct	163 830	324	
Nançay	N	82 Aug	–	–	Very bad interference
Liposthey	LI	82 Aug	237 570	185	
Hendaye	H	82 Aug	–	–	Very bad interference
Palma Mallorca	P	82 Sept	384 620	171	

Table 2. The observations.

Source	Baseline code	Projected baseline (/1000 λ)	Solar elongation (°)	No. of observa-tions	Visibility (arbitrary units)	rms error
3C48	LB	0.1	64	2	106	2
	K	1.35	51	3	90	4
	WC	6.36	60	2	83	4
	S	16.82	72	3	87	4
	CH	33.25	127	3	86	4
	L	50.55	149	4	67	3
	W	67.81	158	5	72	3
	LE	120.20	93	4	66	3
	PA	155.40	159	2	82	4
	LI	229.18	121	3	30	2
	P	375.43	129	4	15	2
3C147	LB	0.1	28	2	83	2
	S	16.83	32	2	75	4
	CH	34.95	80	4	68	3
	L	50.59	142	3	65	4
	W	71.98	122	6	66	3
	LE	121.06	137	1	58	6
	PA	163.23	122	4	58	3
	P	383.91	85	4	19	1
3C216	LB	0.1	38	2	83	2
	K	1.35	49	2	72	4
	WC	6.36	41	4	59	3
	S	16.83	32	4	52	3
	CH	34.56	45	2	41	4
	L	50.58	110	3	<26	–
	W	70.90	86	4	<26	–
	LE	120.95	155	4	<26	–
	PA	161.00	87	4	<26	–
3C380	LB	0.1	108	2	107	2
	K	1.35	107	3	108	4
	WC	6.36	108	2	102	4
	S	16.83	108	2	52	4
	CH	34.92	99	2	38	4
	L	50.59	78	4	<26	–
	W	71.88	84	4	<26	–
	LE	121.07	73	4	<26	–
	PA	162.99	84	3	<26	–

from the Sun in the plots of cross-correlation function with delay, rejecting all measurements which were doubtful. Man-made interference, being uncorrelated at the two ends of the interferometer, was important only if it was so large as to reduce the sensitivity of one or other antenna system. We rejected any measurements which might have been affected by more than about 10 per cent; in fact interference was only a major problem at two sites in France where it made observation impossible. We discuss the effects of the ionosphere and interplanetary medium in the next section.

4 The effects of the ionosphere and the interplanetary medium

Irregularities of electron density in the ionosphere and interplanetary medium introduce phase fluctuations across a wavefront observed on the Earth. Intensity scintillation occurs

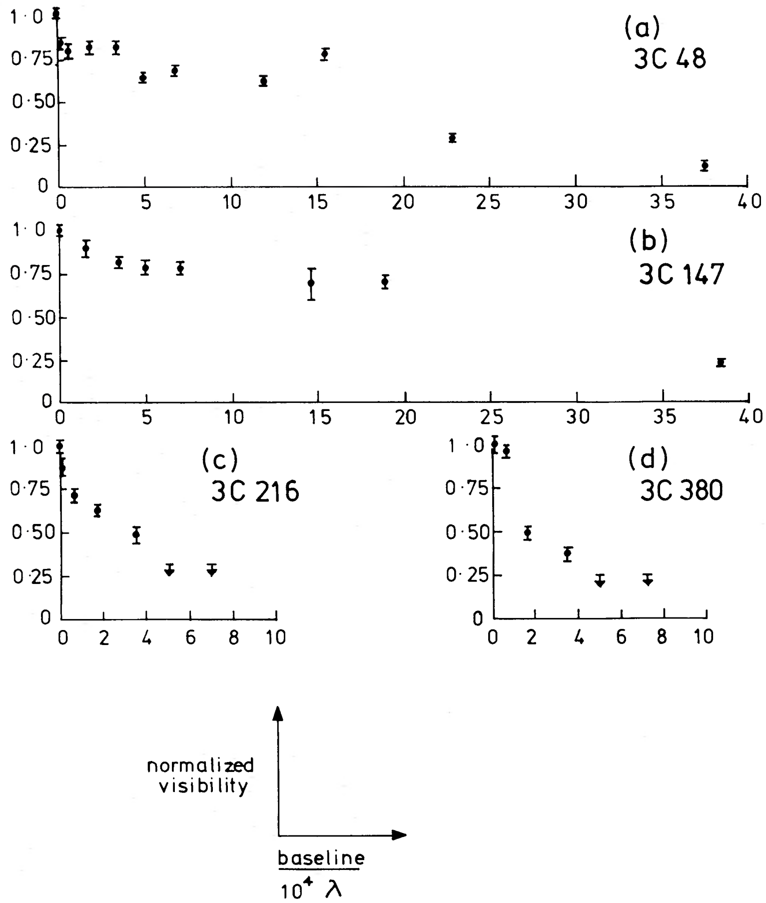

Figure 3. The observed visibilities.

when the irregularities have a scale size, L, which is smaller than the Fresnel scale, $L_f \sim \sqrt{2\lambda z}$, where λ is the wavelength and z is the distance to the scattering layer. Otherwise, the result is simply to introduce random phase deviations in the signal measured by the interferometer. These deviations can cause significant decorrelation of the signal under certain circumstances

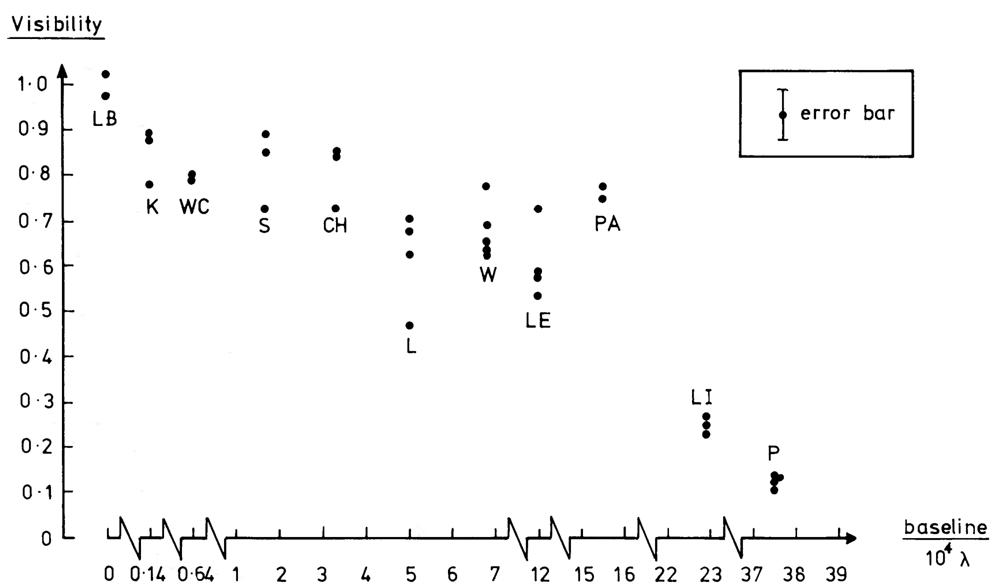

Figure 4. Individual measurements of the visibility of 3C 48 to show their day-to-day consistency. The error bar indicates the rms deviation in one measurement.

which depend upon the baseline length, D, the power spectrum of the electron density irregularities in the medium, the coherent integration time of the observation, and the velocity, V, with which the medium is moving across the line-of-sight to the radio source.

Gapper & Hewish (1981) have plotted the power spectrum of the phase fluctuations at 81.5 MHz caused by the interplanetary medium under normal conditions, when the line-of-sight to the radio source passes the Sun at a distance $p = 0.5$ AU (equivalent to a solar elongation $\epsilon = 30°$). The spectrum, $P_\phi(L)$, may be approximated by

$$\phi_0^2 P_\phi(L) = 4.55 \times 10^{-9} L^{8/3} \text{ rad}^2 \text{ Hz}^{-1},$$

where L is expressed in km, and ϕ_0 (rad) is the rms phase deviation. (We have assumed a mean value of $V = 400 \text{ km s}^{-1}$.) Scale lengths larger than D cause a shift in the apparent position of the radio source and hence a deviation of the observed fringe rate from its theoretical value. Such deviations are allowed for at the fringe-stopping stage, as explained in Section 2. We therefore adopt D as the largest scale length which might contribute to decorrelation of the signal. (The time-scale of fluctuations thus associated with our largest baseline was less than the integration time of the observations.) Readhead, Kemp & Hewish (1978) have shown that ϕ_0 varies as $p^{-1.5}$ so we deduce that

$$\phi_0 = 3.69 \times 10^{-4} p^{-1.5} D^{5/6} \text{ rad},$$

where D is expressed in km and p in AU. The decorrelation exceeds 5 per cent only for $\phi_0 > 0.3$ rad, corresponding at $D = 1500$ km to $p < 0.67$ ($\epsilon < 42°$). We therefore conclude that interplanetary scintillations had negligible effect on our observations.

Large-scale (~ 100 km) irregularities in the ionosphere also cause the observed fringe rate to deviate from its theoretical value. On the assumption of a total electron content of the ionosphere between 5×10^{16} and $5 \times 10^{17} \text{ m}^{-2}$ (Hagfors 1976), the observed variations in fringe rate were consistent with fractional changes in the ionosphere of between 1 and 10 per cent on a time scale of 15 min, values which are in excellent agreement with those obtained by other authors (e.g. Bougeret 1981). Such irregularities are also responsible for the differential Faraday rotation.

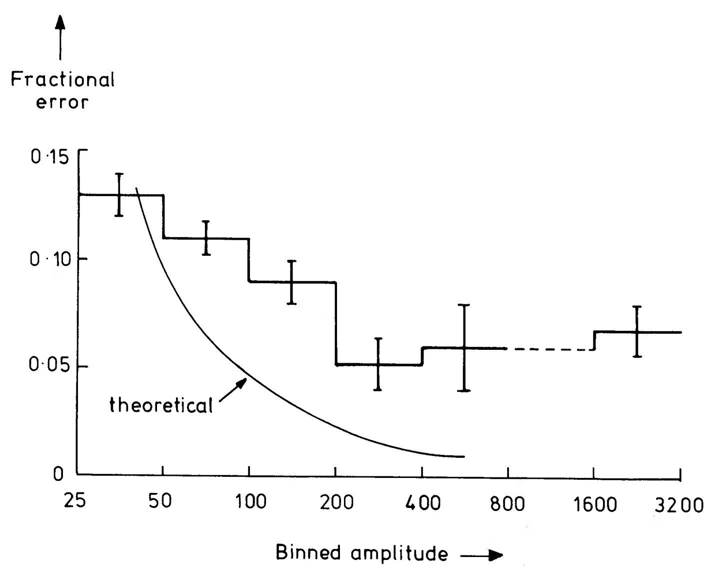

Figure 5. The measured fractional error (histogram) plotted as a function of the amplitude of the correlated signal. The theoretical error, expected in the absence of scintillations, is shown by the solid curve.

Smaller scale (~ 5 km) irregularities in the ionosphere cause scintillation which can be severe enough to cause decorrelation of the interferometer signal. If we approximate the ionosphere by a slab of plasma 100 km thick, and assume a Gaussian autocorrelation function for the density irregularities in the medium (Rufenach 1972), the visibility of a point source will be reduced by 5 per cent when the electron-density variations exceed about $10^9\,m^{-3}$. The work by Crane (1977) suggests that less than 1 in 10 of our observations would have been affected to this extent. However, we did observe complete loss of signal on a few occasions at the longest baselines, which we ascribe to abnormal ionospheric activity.

Another effect of scintillation of either variety is that it increases the noise associated with any measurement. This is illustrated in Fig. 5 where the measured fractional error has been plotted against the fringe amplitude averaged into logarithmic bins. The expected variation if the error is due entirely to statistical fluctuations in the measurements themselves is shown by the solid curve; the fact that the apparent error seemed never to drop below about 6 per cent suggests that this amount was always contributed by scintillation when averaged over 100 s. Note that this implies a decorrelation of less than 4 per cent.

Scattering in the interstellar medium produces a fluctuating signal at the Earth only if the radio source has an angular size of not more than a few milliarcsec and if a very narrow bandwidth is used. Otherwise, the radiation is scattered into an angle of about $\theta_s = 0.15/(\sin|b|)^{1/2}$ arcsec at 81.5 MHz (Duffett-Smith & Readhead 1976) where b is the galactic latitude. Thus we do not expect interstellar scattering to affect our results for sources with $|b| > 10°$ unless the baseline is greater than about 1500 km.

5 The results

We now discuss our measurements of the four sources and deduce what we can about the gross features of their structure at 81.5 MHz, aided by data from synthesis telescopes at higher frequencies. We generally assume circular symmetry as our sparse coverage of the $u-v$ plane does not justify more elaborate assumptions to be made.

3C 48

VLA, 5 GHz: Calibrator list – extended structure on a scale of about 2 arcsec contributes less than 2 per cent of the total flux density.

VLA, 15 GHz: Single component 0.5 arcsec north–south but narrower east–west (J. Peacock, in preparation).

LBI, 408 MHz: An elliptical Gaussian model 0.35 by ≤ 0.23 arcsec fits the visibility data from a single baseline of $18 \times 10^4\,\lambda$ (Anderson & Donaldson 1967).

LBI, 81.5 MHz: (Fig. 3a): The visibility curve shows a drop of ~ 15 per cent within the first step of 1400 λ, indicating structure on scales greater than 1 arcmin. Confusion due to nearby sources is not likely to produce a decrease of more than 5 per cent, and ionospheric decorrelation is probably negligible since both measurements were made during the afternoon. Similar observations of 3C 27 made on the same days show no such decrease. Further evidence for large-scale structure comes from Russian 85-MHz radio-linked interferometry (Vasiljev *et al.* 1976). Normalized plots of the visibilities measured by them and us are superimposed in Fig. 6(a). The data are consistent within the errors and a significant downward trend is evident. That part of the visibility curve extending from 1400 to 170 000 λ may be interpreted in terms of an extended component contributing about 15 per cent of the total flux density and about 3.5 arcsec across, together with a compact component about 0.5 arcsec in extent contributing about 70 per cent of the total flux density.

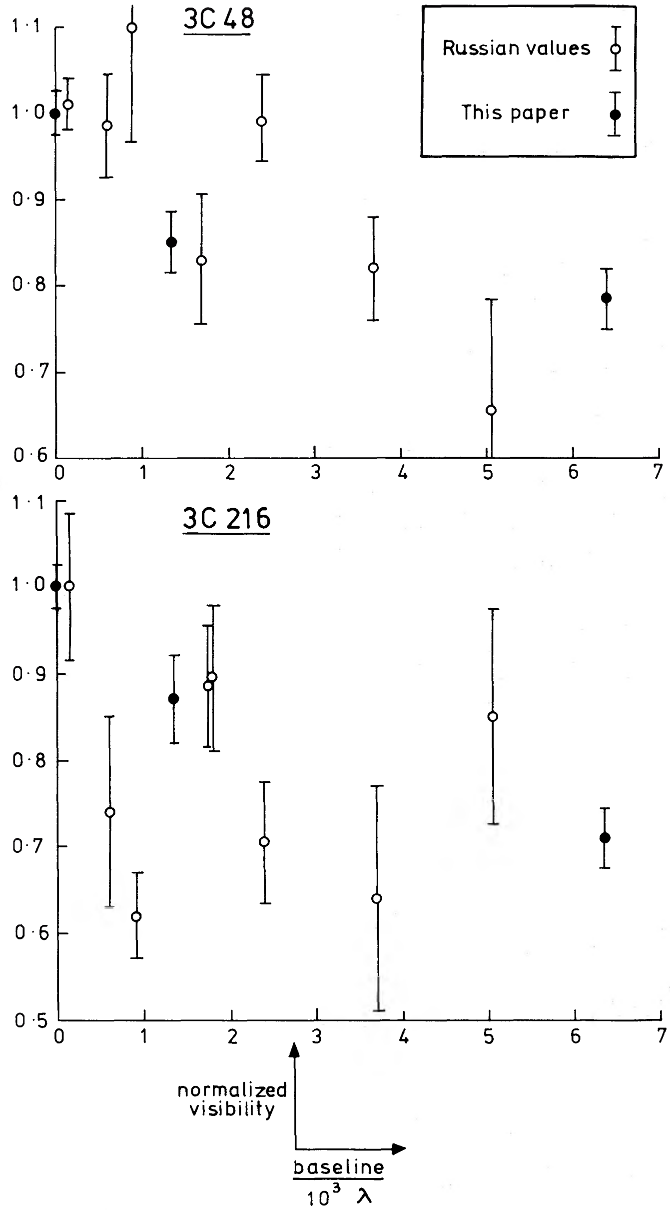

Figure 6. Comparison of visibilities measured by Vasiljev *et al.* (1976) at 85 MHz (open circles) and by ourselves at 81.5 MHz (filled circles) for (a) 3C 48 and (b) 3C 216.

3C 147

VLA, 1.4 GHz: Calibrator list – extended structure on a scale greater than 2 arcsec contributes 2–5 per cent to the total flux density.

LBI, 408 MHz: An elliptical Gaussian model 0.52 by $\leqslant 0.21$ arcsec fits the visibility data from a single baseline of $18 \times 10^4 \lambda$ (Anderson & Donaldson 1967).

LBI, 81.5 MHz: (Fig. 3b): The fit of a simple core-halo Gaussian model to our measurements implies a compact component of 0.4 arcsec diameter (to $1/e$) contributing 80–85 per cent of the total emission, together with an extended component about 4 arcsec in size contributing the remaining emission.

3C 216

VLA, 5 GHz: Three components of about 2 arcsec total extent aligned along PA 45° (Schilizzi, Kapahi & Neff 1982).

LBI, 81.5 MHz: (Fig. 3c): There is evidence for two extended components, one about 3 arcsec in extent contributing up to 70 per cent of the total flux density (though IPS reveals a compact component), and the other about 1 arcmin in extent, contributing up to 30 per cent of the total emission. The Russian LBI observations at 85 MHz (Vasiljev *et al.* 1976) are shown in Fig. 6b; although the quality of the data is poor, there is nevertheless a downward trend. We have checked the 6C records for confusing sources at 151 MHz but can account for a drop of no more than 10–15 per cent of the total flux density in this way, although the interferometer beam shape is not accurately known. Ionospheric decorrelation is negligible.

3C 380

MERLIN 1666 MHz: Extended structure on a scale of ~ 6 arcsec (Wilkinson 1982).

LBI, 81.5 MHz: (Fig. 3d): The visibility falls off rapidly with increasing east–west baseline, indicating extended structure on a scale of 6–7 arcsec contributing about half of the total emission. The point at 35 000 λ indicates that a north-east to south-west cut across the source is probably narrower than an east–west cut, consistent with the orientation seen at 1666 MHz.

The four radio sources discussed here are all quasars and compact at high frequencies, yet show strong evidence for extended structure in our measurements at 81.5 MHz. The largest structures in 3C 48 and 216 have linear sizes of more than 350 and 450 kpc respectively ($H_0 = 50\,\mathrm{km\,s^{-1}\,Mpc^{-1}}$; $q_0 = 0.5$). These and the results for the other sources in our sample will be discussed in detail elsewhere.

Future long-baseline observations at 81.5 MHz will be made with the 9000-m^2 parabolic trough antenna which can track radio sources for about 3 hr either side of the meridian in order to obtain greater u–v coverage. NRAO Mk II type VLBI recording and playback systems will be used and we shall be able to study extended structure in some detail. Unless we can include a second large antenna in the observations we shall be unable to use 'closure' phase in constructing maps, but it is already clear that LBI measurements at metre wavelengths can provide important new information about radio source structure.

Acknowledgments

This experiment would have not been possible without the assistance of a great many people. We thank especially members of the assistant staff and research students at the Mullard Radio Astronomy Observatory, Dr D. M. A. Wilson who designed the portable antenna and trailer, and those hospitable and patient people who accommodated our equipment on their property or assisted us on our way, including: Professor and Mrs A. Hewish, Mrs B. Ford, Mr J. Jewers, Mr and Mrs C. Vincent-Smith, the Steward of Christ's Hospital, Mr R. Meredith, Mr J. R. Welford, Mr and Mrs Knowles, Mrs McCorquodale, Dr A. Boischot, Dr F. Genova, the Director of the Station de Radio-astronomie de Nançay, Dr J. de la Noë, M. M. Leveque, M. R. Lauqué, M. M. Tellechea, the Director of the French Academy of Sciences, Dr and Mrs J. C. Rushton, Sn M. M. Bosch and Mrs P. M. Duffett-Smith. JSH and WGR gratefully acknowledge receipt of SERC studentships. We also thank A. Purvis and L. Miller for illuminating discussions, and an anonymous referee for helpful comments.

References

Allen, L. R., Anderson, B., Conway, R. G., Palmer, H. P., Reddish, V. C. & Rowson, B., 1962. *Mon. Not. R. astr. Soc.*, **124**, 477.

Anderson, B. & Donaldson, W., 1967. *Mon. Not. R. astr. Soc.*, **137**, 81.

Bougeret, J. L., 1981. *Astr. Astrophys.*, **96**, 259.
Clark, T. A., Erickson, W. C., Hutton, L. K., Resch, G. M., Vandenberg, N. R., Broderick, J. J., Knowles, S. H. & Youmans, A. B., 1975. *Astr. J.*, **80**, 923.
Crane, R. K., 1977. *Proc. IEEE*, **65**, 180.
Duffett-Smith, P. J., 1980. *Mon. Not. R. astr. Soc.*, **192**, 33.
Duffett-Smith, P. J., Purvis, A. & Hewish, A., 1980. *Mon. Not. R. astr. Soc.*, **190**, 891.
Duffett-Smith, P. J. & Readhead, A. C. S., 1976. *Mon. Not. R. astr. Soc.*, **174**, 7.
Gapper, G. R. & Hewish, A., 1981. *Mon. Not. R. astr. Soc.*, **197**, 209.
Hagfors, T., 1976. *Methods in Experimental Physics*, Vol. 12b, p. 119, Academic Press Inc., New York.
Laing, R. A., 1981. *Mon. Not. R. astr. Soc.*, **194**, 301.
Lonsdale, C. J. & Morison, I., 1980. *Nature*, **288**, 66.
Perley, R. A., 1982. *Astr. J.*, **87**, 859.
Readhead, A. C. S. & Hewish, A., 1974. *Mon. Not. R. astr. Soc.*, **78**, 1.
Readhead, A. C. S., Kemp, M. C. & Hewish, A., 1978. *Mon. Not. R. astr. Soc.*, **185**, 207.
Rufenach, C. L., 1972. *J. Geo. Res.*, **77**, 4761.
Schilizzi, R. T., Kapahi, V. K. & Neff, S. G., 1982. *J. Astrophys. Astr.*, **3**, 173.
Vasiljev, M. Yu, Volodin, Yu. V., Gubanov, A. G., Dagkesamanskaja, R. D., Dagkesamanskii, G. I., Dobish, G. I., Ivanov, V. V., Izvekov, B. K., Sukhodolskii, S. A. & Frolov, V. A., 1976. *Moscow Acad. Sci.*, preprint number 179.
Wilkinson, P. N., 1982. *Extragalactic Radio Sources, IAU Symp. No. 97*, eds D. S. Heeschen & C. M. Wade, Reidel, Dordrecht, Holland.
Winter, A. J. B., Wilson, D. M. A., Warner, P. J., Waldram, E. M., Routledge, D., Nicol, A. T. N., Boysen, R. C., Bly, D. W. J. & Baldwin, J. E., 1980. *Mon. Not. R. astr. Soc.*, **192**, 931.